Preclinical SPECT/CT Imaging of αvβ6 Integrins for Molecular Stratification of Idiopathic Pulmonary Fibrosis

Alison E. John[1], Jeni C. Luckett[2], Amanda L. Tatler[1], Ramla O. Awais[3], Ami Desai[4], Anthony Habgood[1], Steve Ludbrook[5], Andy D. Blanchard[5], Alan C. Perkins[3], R. Gisli Jenkins*[1], and John F. Marshall*[4]

[1]Nottingham Respiratory Research Unit, University of Nottingham, Nottingham, United Kingdom; [2]Centre for Biomolecular Sciences, University of Nottingham, Nottingham, United Kingdom; [3]Radiological and Imaging Sciences, University of Nottingham, Nottingham, United Kingdom; [4]Institute of Cancer, Queen Mary, University of London, London, United Kingdom; and [5]GlaxoSmithKline, Stevenage, United Kingdom

Transforming growth factor β activation by the αvβ6 integrin is central to the pathogenesis of idiopathic pulmonary fibrosis. Expression of the αvβ6 integrin is increased in fibrotic lung tissue and is a promising therapeutic target for treatment of the disease. Currently, measurement of αvβ6 integrin levels in the lung requires immunohistochemical analysis of biopsy samples. This procedure is clinically impractical for many patients with pulmonary fibrosis, and a noninvasive strategy for measuring αvβ6 integrin levels in the lungs is urgently required to facilitate monitoring of disease progression and therapeutic responses. **Methods:** Using a murine model of bleomycin-induced lung injury, we assessed the binding of intravenously administered ^{111}In-labeled αvβ6-specific (diethylenetriamine pentaacetate-tetra [DTPA]-A20FMDV2) or control (DTPA-A20FMDVran) peptide by nanoSPECT/CT imaging. Development of fibrosis was assessed by lung hydroxyproline content, and αvβ6 protein and *itgb6* messenger RNA were measured in the lungs. **Results:** Maximal binding of ^{111}In-labeled A20FMDV2 peptide to αvβ6 integrins was detected in the lungs 1 h after intravenous administration. No significant binding was detected in mice injected with control peptide. Integrin binding was increased in the lungs of bleomycin-, compared with saline-, exposed mice and was attenuated by pretreatment with αvβ6-blocking antibodies. Levels of ^{111}In-labeled A20FMDV2 peptide correlated positively with hydroxyproline, αvβ6 protein, and *itgb6* messenger RNA levels. **Conclusion:** We have developed a highly sensitive, quantifiable, and noninvasive technique for measuring αvβ6 integrin levels within the lung. Measurement of αvβ6 integrins by SPECT/CT scanning has the potential for use in stratifying therapy for patients with pulmonary fibrosis.

Key Words: integrin αvβ6; fibrosis; SPECT/CT

J Nucl Med 2013; 54:2146–2152
DOI: 10.2967/jnumed.113.120592

Idiopathic pulmonary fibrosis (IPF) is a chronic, progressive, fibrotic lung disease associated with serious morbidity, premature death, and a median survival of less than 3 y (*1*). The incidence has risen steadily for the last few decades (*1,2*), and the 5-y survival rate is worse than most cancers (*3*). Although novel drug-based therapies such as *N*-acetyl cysteine (*4*) and Pirfenidone (Intermune) (*5*) have shown encouraging responses in clinical trials, to date, no therapy has successfully modified the disease course.

The management of IPF is complicated by the heterogeneous nature of the condition, with considerable variability in the clinical course, and the absence of good biomarkers of disease progression or therapeutic response (*6*). Even using the latest diagnostic imaging such as high-resolution CT and pathologic characterization according to American Thoracic Society/European Respiratory Society criteria (*7*), it is difficult to distinguish chronic stable, progressive, or life-threatening acutely deteriorating fibrosis before it becomes self-evident.

With burgeoning data on the pathogenesis of IPF (*8*), heterogeneity of clinical course (*9*), expense of novel therapies, and potential adverse effects of ineffective therapies (*10*), the development of a stratified approach to the management of IPF is urgently required. Such an approach requires companion diagnostic tests to select patients for therapeutic intervention, excluding those unlikely to respond. There are currently no reliable measures to stratify patients with IPF. Although longitudinal declines in lung function (*11–14*), extensive fibrosis, and honeycombing on high-resolution CT imaging are associated with worsening mortality, they give little information on pathogenesis or likely response to therapy. Molecular and histopathologic stratification is well established in cancer studies (*15–17*), but attempts to stratify IPF on the basis of histopathologic or molecular phenotyping have been unconvincing (*18,19*). Furthermore, the high mortality rate associated with video-assisted thoracoscopic surgical biopsy and the lack of longitudinal sample collection makes histopathologic phenotyping in IPF problematic. Serum and bronchoalveolar lavage biomarkers with the potential to stratify IPF patients have been identified, including KL-6, surfactant protein A and D, CCL18, and MMP7 (*20*); however, none has been validated longitudinally or in response to therapy.

The use of nuclear imaging in IPF is an emerging strategy for disease stratification. Initial studies have used PET tracers including ^{18}F-FDG and ^{68}Ga-labeled somatostatin analogs that bind the somatostatin receptor (*21,22*). Pulmonary uptake of both these radiotracers is increased in IPF patients, and lung ^{18}F-FDG levels have been related to disease severity (*23*). Although there are some preclinical data demonstrating a role for somatostatin receptors in IPF (*24*), neither of these tracers targets well-validated pathways implicated in IPF.

The αvβ6 integrin has been implicated in multiple models of lung fibrosis (*25–27*), as well as being upregulated in patients with IPF (*27,28*), and there is some evidence to suggest that levels may

Received Jan. 25, 2013; revision accepted Jul. 16, 2013.
For correspondence or reprints contact: Gisli Jenkins, Nottingham Respiratory Research Unit, University of Nottingham, Clinical Sciences Building, City Hospital, Hucknall Rd., Nottingham, NG5 1PB U.K.
E-mail: Gisli.jenkins@nottingham.ac.uk
*Contributed equally to this work.
Published online Oct. 28, 2013.

vary between patients with differing interstitial lung diseases (*28*). Targeting this molecule has considerable therapeutic potential (*25, 28*), and a clinical trial is currently in progress (NCT01371305; ClinicalTrials.gov). To date, measurement of αvβ6 levels in fibrotic lung tissue has been restricted to the detection of the integrin by immunohistochemistry (*27,28*). Therefore, we developed a strategy for detecting the αvβ6 integrin in vivo using an imaging technique with a peptide derived from the VP1 coat protein of the foot-and-mouth disease virus. The A20FMDV2 peptide shows highly selective αvβ6 ligand binding activity and is 1,000-fold more selective for αvβ6 than for other arginine-glycine-aspartate (RGD)–binding integrins ($\alpha_v\beta_3$, αvβ5, and α5β1) (*29*). αvβ6-expressing human pancreatic (*30*) and breast (*31*) cancer cells have been imaged by PET or SPECT scanning in murine models using radiolabeled A20FMDV2; however, there are no reports measuring endogenous αvβ6 levels in vivo. This ^{111}In-labeled αvβ6 integrin–specific peptide can monitor and predict the development of lung fibrosis in a bleomycin model of disease using SPECT. These are the first studies, to our knowledge, to noninvasively measure a well-validated molecular target in IPF, and our data describe a strategy that has the potential both to facilitate stratification of treatment and to identify a potential prognostic biomarker in IPF.

MATERIALS AND METHODS

Peptide Synthesis, Radiolabeling, and Radiochemical Analysis

DTPA-A20FMDV2 (αvβ6-specific) and DTPA-A20FMDVran (random control) peptides were synthesized with biotinyl lysine at position 2 by the Cancer Research U.K. Peptide Synthesis Laboratory using standard fluoroenylmethyloxycarbonyl (FMOC) solid-phase peptide synthesis (SPPS) protocols and conjugated with the chelating agent diethylenetriamine pentaacetate-tetra (DTPA) at the N terminus. Detailed methods for the synthesis and radiolabeling of both peptides are described in the supplemental data (supplemental materials are available at http://jnm.snmjournals.org).

Both test and control peptides were purified by high-performance liquid chromatography to give greater than 95% purity and lyophilized (Supplemental Fig. 1). Peptide stock solutions were prepared in metal-free water, and standard concentrations were confirmed spectrophotometrically using absorption at 215 nm. The radiolabeling of both peptides was performed as previously described by Saha et al. (*25*).

After radiolabeling, the average activity in each 5-μg aliquot of ^{111}In-DTPA-A20FMDV2 or ^{111}In-DTPA-A20FMDVran across all studies was 28.70 MBq (range, 16.53–34.6 MBq) and 26.26 MBq (range, 17.2–32.1 MBq), respectively. Specific activity ranged from 9.33 to 19.54 MBq per nanomole.

In Vivo Studies

Male 6-wk-old C57BL/6 mice received 60IU bleomycin or saline via oropharyngeal dosing, as previously described (*32*), before nanoSPECT/CT imaging and image analysis. For integrin-blocking experiments in mice exposed to bleomycin or saline 4 wk previously, animals received either anti-αvβ6 (10D5; Millipore) or IgG2a isotype control antibody at a dose of 2.5 mg/kg, 24 h before nanoSPECT/CT imaging. All mice were housed under specific pathogen-free conditions, and animal studies were ethically reviewed and performed at the University of Nottingham in accordance with the Animals (Scientific Procedures) Act 1986, institutional animal care and use regulations, and GSK Policies on the Care, Welfare and Treatment of Animals.

NanoSPECT/CT Imaging Studies

Whole-body helical CT and SPECT scans were obtained with a nanoSPECT/CT imaging system (Bioscan Inc.) fitted with 4 tungsten collimators and nine 1.4-mm-diameter pinholes. SPECT images were obtained with a time per view of 60 s, resulting in a scan time of 30–45 min. CT images were obtained using a tube voltage of 45 kVp and an exposure time of 500 ms per view. Mice were injected intravenously via the tail vein with 5 μg of ^{111}In-DTPA-A20FMDV2 or control ^{111}In-DTPA-A20FMDVran peptide in a 50-μL volume before nanoSPECT/CT imaging. Mice were anesthetized by 3% isoflurane inhalation and maintained at 1%–1.5% for the duration of scanning. The mice were placed in a tail-first prone position, in a Minerve (Siemens) air-warmed chamber, and breathing rates were monitored. After data collection, CT and SPECT images were coregistered, and image analysis performed using InVivoScope molecular imaging software (Bioscan Inc.). For analysis of peptide binding specifically, a region of interest (ROI) was manually created from the CT scans to create a 3-dimensional volumetric dataset. This 3-dimensional ROI was subsequently overlaid with a semiautomatic ROI in which global thresholding was applied to identify only voxels within the density range (−1,000 to +100) that includes normal and diseased mouse lung tissue (*33*). The activity in megabecquerels was then recorded in voxels found within the lung ROI for each mouse. Data are expressed as percentage of the initial activity of ^{111}In-labeled peptide administered by intravenous injection. During image processing, the scales for cross-sectional images and reconstructed 3-dimensional movies were identical for all CT (76%–8%) and SPECT (86%–12%) images presented. To determine the optimal time for in vivo imaging of the αvβ6 integrin, binding of the targeted and control peptides was assessed by whole-body nanoSPECT/CT imaging either 1 or 3 h after peptide injection. The highest signal intensity was observed in the lungs 1 h after injection (Supplemental Fig. 2); therefore, this time point was used in experimental protocols.

Hydroxyproline Assay

The hydroxyproline content of the mouse lung was measured using standard methodology previously described by Woessner et al., with some modifications (*25*). Briefly, after perfusion with phosphate-buffered saline, lungs were ground to fine powder under liquid nitrogen. Samples were mixed with tricarboxylic acid (50%; Sigma Chemical Co.), incubated on ice, and baked overnight in 12N hydrochloric acid. Samples were then reconstituted with distilled water and added to 1.4% chloramine T (Sigma Chemical Co.) in 10% isopropanol and 0.5 M sodium acetate for 20 min. Erlich solution (Sigma Chemical Co.) was added and incubated at 65°C for 15 min before absorbance was measured at 550 nm

Immunohistochemical Staining and Evaluation

After SPECT/CT scanning, lungs were formalin-fixed and paraffin-embedded before staining with 6.2G2 (anti-αvβ6; a kind gift from Biogen Idec) using a mouse-on-mouse kit (M.O.M. Kit; Vector Labs Inc.) after pepsin antigen retrieval as previously described (*31*). Immunohistochemical scoring was performed to assess the percentage of epithelial cells expressing αvβ6 across the tissue sections. Images were captured using a Nikon Eclipse 90i microscope and NIS Elements AR3.2 software (Nikon). For each set of lungs, 5 random fields were captured at ×10 magnification and overlaid with a grid containing 192 squares of 50 μm^2. The number of squares containing αvβ6-positive epithelial cells was recorded and after exclusion of any boxes that contained no cells, the percentage of the lung tissue containing αvβ6-positive epithelial cells was determined—that is, positive stained squares/(total squares − empty squares) × 100.

RNA Isolation and Analysis of Gene Expression

RNA isolation and real-time polymerase chain reaction (RT-PCR) amplification was performed as previously described (*34*) using the MX3000P RT-PCR system (Agilent Technologies) to assess expression of the murine or human β6 integrin (*itgb6*/ITGB6) and murine hypoxanthine-guanine phosphoribosyltransferase (*hprt*) or $\beta_2$microglobulin

(β_2m), as housekeeping genes. Primer sequences are shown in Supplemental Table 1.

Patient Population

Human tissue was obtained after informed consent and institutional ethical review (ethical approval no.: Nottingham Respiratory Research Unit 08/H0407/1).

Statistical Analysis

All data are expressed as mean ± SE of *n* observations. A Student *t* test was used for comparisons between 2 groups and 1-way ANOVA with Bonferroni post hoc multiple-comparisons test for greater than 2 groups. All analyses, including linear regression analysis, were conducted using GraphPad Prism (version 5.04; GraphPad Software).

RESULTS

Binding of αvβ6-Specific Radiolabeled Peptide in Fibrotic Lungs

The level of ^{111}In-DTPA-A20FMDV2 and ^{111}In-DTPA-A20FMDVran uptake in the lungs of mice 28 d after instillation with bleomycin or saline was compared by whole-body nanoSPECT/CT imaging 1 h after intravenous administration of the radiolabeled peptide. Both saline- (Fig. 1A; Supplemental Video 1) and bleomycin- (Fig. 1B; Supplemental Video 2) instilled mice exposed to the αvβ6-binding ^{111}In-DTPA-A20FMDV2 peptide had detectable levels of uptake in the lungs 1 h after administration. In contrast, mice exposed to the ^{111}In-DTPA-A20FMDVran control peptide after saline (Supplemental Video 3; Supplemental Fig. 3A) or bleomycin (Supplemental Video 4; Supplemental Fig. 3B) treatment had low levels of uptake. Mice instilled with bleomycin showed the highest level of retention of the radiolabeled peptide (Fig. 1B), which predominantly overlay areas of lung damage detected on the CT images (Fig. 1D). Peptide binding was also detected in the lungs of saline-treated mice (Fig. 1A), although this showed lower levels of uptake and was not associated with areas of lung damage (Fig. 1C).

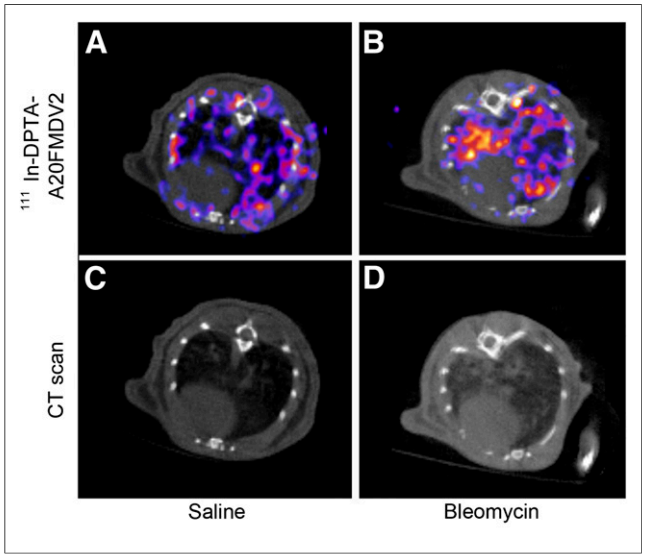

FIGURE 1. Binding of ^{111}In-DTPA-A20FMDV2 peptide in lungs of fibrotic mice was detected at low level in lungs of saline-treated mice (A) with no evidence of parenchymal damage on the corresponding CT scans (C). Level of ^{111}In- DTPA-A20FMDV2 binding was greatly increased in bleomycin-treated animals (B), which showed clear evidence of parenchymal damage in axial CT scans (D).

Quantification of peptide retention in the lungs, expressed as percentage of the initial activity of ^{111}In-labeled peptide administered, demonstrated that bleomycin-treated mice had significantly increased levels of ^{111}In, compared with saline-treated control mice (Fig. 2). Although a low level of ^{111}In was detected in mice receiving the ^{111}In-DTPA-A20FMDVran control peptide, there was no significant difference in the amount of radioactivity seen in bleomycin- or saline-treated mice, and it was significantly lower than that detected in the lungs of saline-instilled ^{111}In-DTPA-A20FMDV2 peptide–exposed mice.

Attenuation of αvβ6 Integrin Signal by αvβ6 Integrin–Blocking Antibody

To confirm that ^{111}In-DTPA-A20FMDV2 binding in the lung was a specific interaction between peptide and the αvβ6 integrin, and that a change in signal intensity could be detectable in response to a therapy, mice were treated with an αvβ6-blocking antibody 24 h before injection with the radiolabeled peptide. Scans of the upper torso in bleomycin-treated mice receiving IgG2a isotype control antibody clearly showed binding of ^{111}In-DTPA-A20FMDV2 in the lungs and submandibular glands (Supplemental Fig. 4A; Supplemental Video 5). In contrast, pretreatment with an αvβ6-blocking antibody led to a reduction in the level of radioactivity detected in all areas of the scan (Supplemental Fig. 4B; Supplemental Video 6). The signal attenuation was particularly apparent in cross-sectional scans of the lungs from bleomycin-instilled mice pretreated with anti-αvβ6–blocking antibodies (Fig. 3A), compared with the IgG2a isotype control antibody (Fig. 3B). The radioactive signal in saline-instilled, ^{111}In-DTPA-A20FMDV2–exposed, animals was similarly reduced in response to the αvβ6-blocking antibody (Fig. 3C) when compared with IgG2a-treated mice (Fig. 3D). Quantification of the level of radiolabeled peptide in the lungs confirmed that bleomycin-induced lung fibrosis leads to enhanced binding, compared with saline-instilled mice, and this binding can be significantly inhibited in the presence of an αvβ6-blocking antibody in both saline- and bleomycin-treated lungs (Fig. 4).

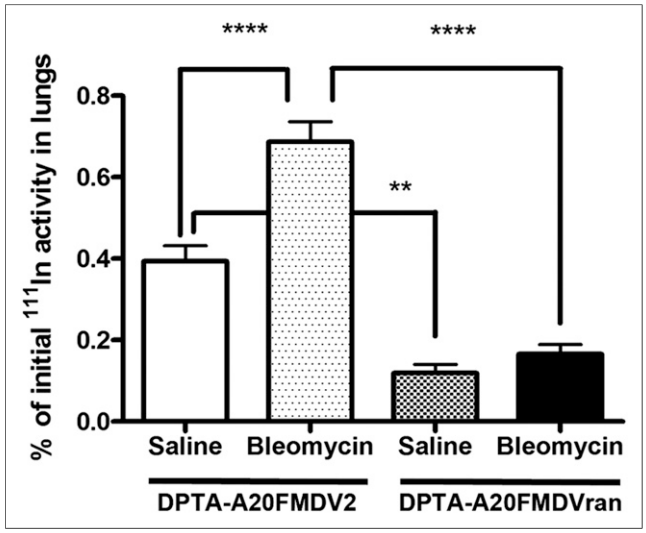

FIGURE 2. Levels of binding in lungs, expressed as percentage of initial activity of ^{111}In-labeled peptide, were compared in bleomycin- (n = 18) and saline- (n = 8) treated mice. Binding of ^{111}In-DTPA-A20FMDVran peptide in lungs of saline- (n = 6) or bleomycin- (n = 8) treated mice was also assessed. Data are presented as mean ± SEM. ****$P < 0.0001$. **$P < 0.01$.

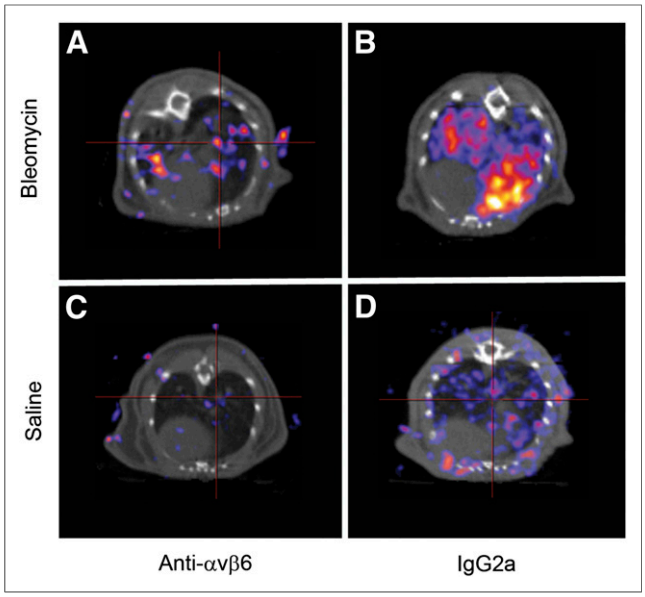

FIGURE 3. Axial SPECT/CT scans of thorax detected binding of ^{111}In-DTPA-A20FMDV2 in lungs of bleomycin-treated animals receiving αvβ6-blocking antibody (A) or IgG2a isotype control (B) (2.5 mg/kg) 24 h before imaging. Effect of αvβ6-blocking (C) and IgG2a isotype control (D) antibodies on binding of ^{111}In-DTPA-A20FMDV2 was also assessed in saline-treated mice.

Repeated Measurement of ^{111}In-Labeled Peptide Binding to αvβ6 by SPECT/CT

NanoSPECT/CT imaging is a noninvasive technique that has the capacity to monitor changes in integrin expression over time by use of repeated imaging. To determine whether this would be feasible in our experimental system, saline- or bleomycin-instilled mice received an initial injection of the ^{111}In-DTPA-A20FMDV2 after 14 d and uptake of the radiolabeled peptide was measured. Fourteen days later, binding of the ^{111}In-DTPA-A20FMDV2 was again measured after repeated administration of the peptide. At both time points, there was significantly higher binding of the ^{111}In-labeled peptide in the lungs of mice instilled with bleomycin than in saline-treated mice. When the level of peptide uptake was compared at 2 and 4 wk in the saline- and bleomycin-treated animals, there was no significant difference in the mean level of uptake of ^{111}In-labeled peptide detected at either time point. In bleomycin-treated animals, the mean percentage of initial ^{111}In activity in the lungs was 1.01 ± 0.09 at 2 wk, compared with 1.08 ± 0.1 at 4 wk. Similarly, saline-treated animals had a mean percentage of initial ^{111}In activity of 0.39 ± 0.02 at 2 wk, compared with 0.46 ± 0.03 at 4 wk. When data from repeated scans were compared in individual mice, it was found that there was variability in the level of ^{111}In-DTPA-A20FMDV2 peptide binding in the fibrotic lungs, with half the animals showing increased and half reduced levels of binding at the later time point (Fig. 5; Supplemental Figs. 5A and 5B). Levels in the saline-treated mice were similar at 2 and 4 wk (Fig. 5; Supplemental Figs. 5C and 5D).

Correlation of SPECT/CT Measures of Lung αvβ6 Integrins with αvβ6 Protein, *itgb6* Messenger RNA, and fibrotic endpoints

For SPECT/CT imaging to be a useful tool for stratifying IPF therapy, the binding of the radiolabeled peptide must correlate with appropriate biologic endpoints. Immunohistochemical analysis of αvβ6 protein levels in lungs collected immediately on completion of SPECT/CT scanning showed a significant positive correlation between the percentage of αvβ6-positive epithelial cells and the level of ^{111}In-DTPA-A20FMDV2 peptide binding in the lungs (Fig. 6A). The lungs of bleomycin-treated animals contained not only a greater percentage of αvβ6-positive cells than the saline-treated animals, but the intensity of the αvβ6 staining was also higher in the fibrotic lungs (Supplemental Fig. 6). Mice instilled with bleomycin have an increase in lung fibrosis, as measured by lung hydroxyproline levels at 28 d, compared with saline-instilled controls (Supplemental Fig. 7A). Similarly, mice instilled with bleomycin have a trend toward increased *itgb6* messenger RNA levels, as measured by quantitative RT-PCR, compared with control (Supplemental Fig. 7B). However, this is less than the increased levels of ITGB6 messenger RNA observed in samples from patients with IPF when compared with normal lung tissue samples (Supplemental Fig. 7C). When the binding of ^{111}In-DTPA-A20FMDV2 and hydroxyproline were measured in mice 28 d after saline or bleomycin treatment, there was a significant positive correlation between hydroxyproline levels and peptide binding (Fig. 6B). Likewise, when binding of the radiolabeled αvβ6-binding peptide and *itgb6* messenger RNA levels in lung homogenates were compared in similarly treated mice after 4 wk, again there was a significant positive correlation (Supplemental Fig. 7D). We also examined binding of ^{111}In-DTPA-A20FMDV2 2 wk after saline or bleomycin treatment, and then after 2 additional weeks, we measured hydroxyproline and *itgb6* levels in lung homogenates. There was a weak positive, but nonsignificant, correlation between binding of ^{111}In-DTPA-A20FMDV2 at 14 d after bleomycin instillation and *itgb6* messenger RNA levels at 28 d (data not shown). More importantly, however, there was a significant correlation between ^{111}In-labeled peptide binding at 14 d with the level of hydroxyproline measured in lung homogenates after 28 d (Fig. 6C).

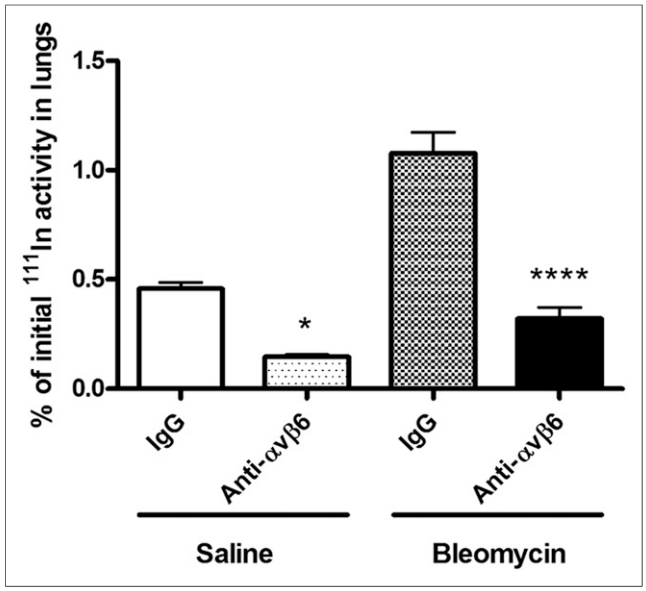

FIGURE 4. Levels of binding in lungs, expressed as percentage of initial activity of ^{111}In-labeled peptide were quantified in saline- (n = 6) or bleomycin- (n = 5) treated animals pretreated with αvβ6-blocking antibody or mice pretreated with IgG2a isotype control (n = 4/group). Data are presented as mean ± SEM. *P < 0.05. ****P < 0.0001.

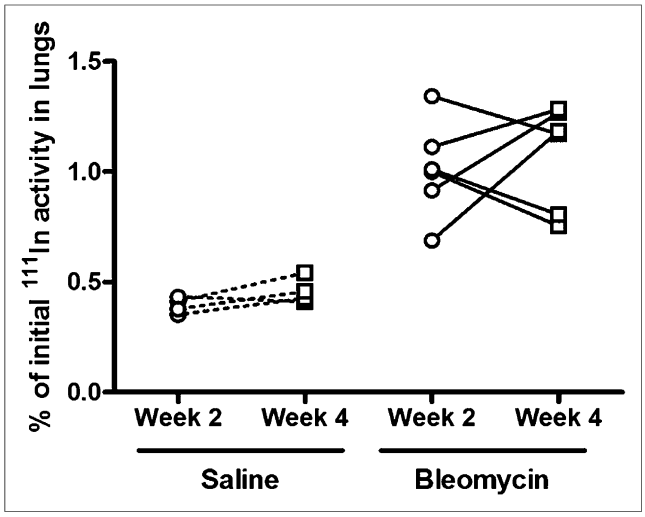

FIGURE 5. Binding of ^{111}In-DTPA-A20FMDV2 to αvβ6 integrins was assessed in lungs of bleomycin-instilled mice (n = 6/group) and saline-treated mice (n = 4/group), and levels of peptide binding were compared after repeated scans at 2 and 4 wk after administration.

DISCUSSION

IPF is chronic, progressive lung disease with a prognosis worse than most cancers and with no therapy proven to improve survival. Novel strategies to improve the outcome for these patients are urgently required, and to facilitate a stratified approach to the treatment of IPF it is important to identify a biomarker that reflects relevant biology. The epithelial-restricted integrin αvβ6 is an attractive target for the treatment of IPF because of its important role in regulating integrin-dependent transforming growth factor β activation (*25*), its pathogenic role in several different experimental models of fibrosis (*25,26,28,35–37*), and its increased expression on alveolar epithelial cells in fibrotic areas of lung in patients with IPF (*27,28*). The expression of αvβ6 integrin is temporally and spatially linked to the development of fibrosis, with upregulation of integrin in the alveolar epithelium being detected before the development of fibrosis and persisting within the fibrotic lesions (*26*). This temporal relationship between the increased expression in αvβ6 integrins and the onset of fibrosis may be possible to exploit as a companion biomarker for the stratified treatment of IPF.

This is the first study, to our knowledge, to use an αvβ6-targeted, radiolabeled peptide to identify the endogenous molecule in vivo. The imaging data demonstrate that the αvβ6 integrin is upregulated after 2 wk and high levels are maintained for 4 wk after injury. This finding is consistent with immunohistochemical assessment of the αvβ6 integrin after bleomycin lung injury, which demonstrates that the αvβ6 integrin is upregulated after 10 d (*25*) and high levels are maintained for at least 21 d (*27*). Previous studies have used this imaging strategy to identify the αvβ6 integrin in murine models of breast (*31*) and pancreatic cancer (*30*), which graft tumors into nude mice. It is extremely encouraging that nanoSPECT/CT scanning was able to measure increased binding of ^{111}In-DTPA-A20FMDV2 in injured murine lung because the level of αvβ6 integrin expression and density of abnormal epithelium is much lower than in orthotopic tumor models. Furthermore, it is likely that the radiolabeled peptide uptake will be considerably greater in patients with IPF because we have previously demonstrated higher levels of αvβ6 integrin staining in sections of fibrotic lung taken from patients with IPF than from sections of lung from mice with bleomycin-induced fibrosis (*27*). This would make SPECT imaging an attractive clinical proposition.

It is also interesting to note that the nanoSPECT/CT scanning is able to detect a consistent level of αvβ6 integrin in aerated, uninjured lung, because immunohistochemical analysis of αvβ6 in the lungs often detects little or no expression of the integrin in normal lung tissue (*27,28*). It is known that αvβ6 integrins are expressed on normal airway epithelium because $\alpha v\beta 6^{-/-}$ mice show an inflammatory phenotype even in the absence of lung injury (*25,38*), they are upregulated in vitro, and they can be detected by flow cytometry (*39*). We are confident that the signal we identify in the mice is specific for the αvβ6 integrin because the targeting peptide has been shown to be up to 1,000-fold more selective for binding to αvβ6 than other αv integrins (*31*), there is a significant positive correlation between the αvβ6 levels detected by nanoSPECT/CT and immunohistochemical staining in the same lungs, it correlates with the change in *itgb6* messenger RNA at the same time-point, there is no signal with the random peptide control, and the signal can be blocked by administration of an αvβ6 integrin–specific blocking antibody before SPECT imaging. Thus, SPECT/CT scanning to detect the αvβ6-targeted radiolabeled peptide is both a better global analysis tool for quantification of this integrin than immunohistochemistry or messenger RNA, techniques which are both subject to sampling bias, and also a highly sensitive measure of αvβ6 integrin expression.

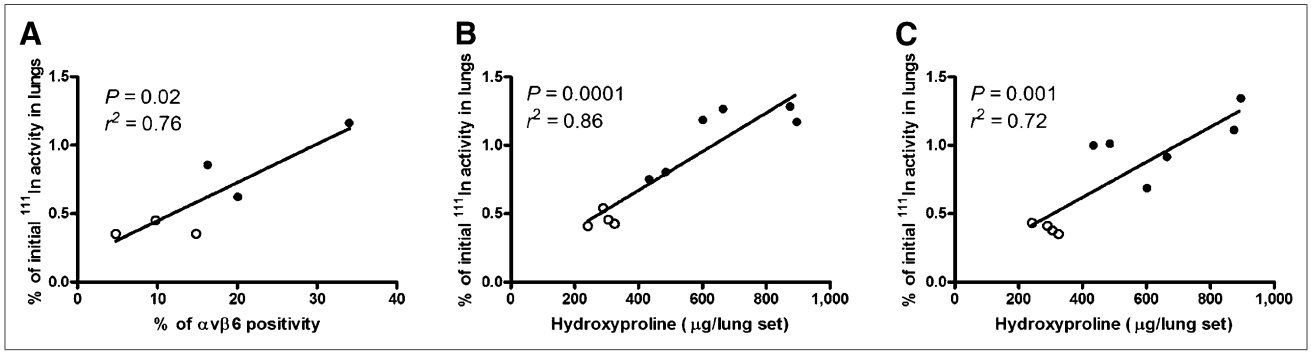

FIGURE 6. Correlation of ^{111}In-DTPA-A20FMDV2 binding within lungs at 28 d after saline (white circles; n = 3) or bleomycin (black circles; n = 3) with epithelial αvβ6 expression in lungs (A). Correlation of ^{111}In-DTPA-A20FMDV2 binding at day 28 (B) and day 14 (C) after saline (n = 4) or bleomycin (n = 6) treatment with lung hydroxyproline levels on day 28.

Although this study focused on the lungs, the nanoSPECT/CT imaging identified uptake of αvβ6 integrin in the submandibular glands and oral cavity and also within the skin. Constitutive αvβ6 expression has previously been reported in salivary glands (*40*) and in the junctional and oral epithelium of the gingival papilla (*41*). Although the role of αvβ6 in salivary glands is unclear, expression in the junctional and oral epithelial cells appears to protect the periodontium from inflammation. This integrin also has a known role in the skin, analogous to its role in the lungs, with the $\alpha v\beta 6^{-/-}$ mice getting increased dermal inflammation (*42*). Furthermore, mice with keratinocyte specific overexpression of the αvβ6 integrin are more prone to dermal fibrosis (*43*), suggesting that SPECT/CT may also have utility in conditions such as systemic sclerosis where there is multiorgan fibrosis. High levels of tracer were detected in the gastrointestinal tracts and kidneys as reported previously (*31*), and although some mice do have αvβ6 on surface colonocytes most of the signal is due to the metabolism and excretion of the radiolabeled peptide (*31*).

The utility of SPECT/CT imaging as a biomarker for stratifying therapy for IPF rests not only on its targeting potential, its sensitivity, and dynamic range—which are demonstrated in the data described—but also through its noninvasive nature and the potential for repeated imaging. At the current time, the only way to detect the αvβ6 integrin in human samples is through immunohistochemical analysis of lung biopsies. Lung biopsies are not universally performed and in the current American Thoracic Society/European Respiratory Society consensus statement are recommended only for discrimination of probable and possible IPF (*7*). As discussed earlier, lung biopsies suffer from sampling bias, leading to suboptimal quantification, and furthermore, given the significant mortality rate associated with lung biopsies, repeated sampling is impractical (*44*). Therefore, molecular imaging using SPECT/CT is likely to offer a significant advance for immunophenotyping patients with IPF that would not otherwise be possible.

These data are likely to be rapidly translatable into clinical practice. The ^{111}In-DTPA-A20FMDV2 is known to bind to human αvβ6 integrins in vitro and in vivo (*30,31*) and ^{111}In-labeled peptides are widely used in clinical practice. Moreover, ^{18}F-A20FMDV2 has been used in vivo for successful PET imaging of αvβ6 on human xenografts (*30*), and PET/CT scans have previously been obtained for IPF patients (*22,23*). Thus, SPECT/CT or PET/CT with radiolabeled A20FMDV2 can offer valuable new imaging modalities for stratifying patients with IPF, although at the present time SPECT is more widely available and less costly than PET imaging.

A potential limitation of this technology in IPF would be the requirement for repeated administration of radiolabeled peptide to patients. In these studies, we administered on average 28.70 MBq of ^{111}In per mouse. For human use, we would anticipate administering approximately 200 MBq for an adult SPECT investigation. In a 70-kg adult with normal renal function, this would equate to the order of 12–16 mSv, a similar amount to that previously received by patients undergoing somatostatin receptor imaging using ^{111}In-octreotide (*45,46*).

CONCLUSION

We have developed a highly sensitive technique for quantifying αvβ6 integrin levels within the lungs. It has a dynamic range sufficient to detect low levels of the integrin in uninjured, normally aerated lungs and in lungs of mice with bleomycin-induced fibrosis. The signal is quantifiable and correlates with the levels of αvβ6 protein, *itgb6* messenger RNA, and hydroxyproline in the lungs. Furthermore, the signal measured at 2 wk is able to predict the degree of fibrosis after 4 wk. This technology may have clinical potential for use in patients with IPF.

DISCLOSURE

The costs of publication of this article were defrayed in part by the payment of page charges. Therefore, and solely to indicate this fact, this article is hereby marked "advertisement" in accordance with 18 USC section 1734. This project was funded by an Medical Research Council MICA project grant (G0901226). No other potential conflict of interest relevant to this article was reported.

ACKNOWLEDGMENTS

We thank Dr. Steve Mather for technical advice and help with radiolabeling and Shelia Violette for providing the anti-αvβ6 antibody for immunostaining.

REFERENCES

1. Gribbin J, Hubbard RB, Le Jeune I, Smith CJ, West J, Tata LJ. Incidence and mortality of idiopathic pulmonary fibrosis and sarcoidosis in the UK. *Thorax.* 2006;61:980–985.
2. Navaratnam V, Fleming KM, West J, et al. The rising incidence of idiopathic pulmonary fibrosis in the UK. *Thorax.* 2011;66:462–467.
3. Vancheri C. Idiopathic pulmonary fibrosis: an altered fibroblast proliferation linked to cancer biology. *Proc Am Thorac Soc.* 2012;9:153–157.
4. Demedts M, Behr J, Buhl R, et al. High-dose acetylcysteine in idiopathic pulmonary fibrosis. *N Engl J Med.* 2005;353:2229–2242.
5. Noble PW, Albera C, Bradford WZ, et al. Pirfenidone in patients with idiopathic pulmonary fibrosis (CAPACITY): two randomised trials. *Lancet.* 2011;377: 1760–1769.
6. Ley B, Collard HR, King TE Jr. Clinical course and prediction of survival in idiopathic pulmonary fibrosis. *Am J Respir Crit Care Med.* 2011;183:431–440.
7. Raghu G, Collard HR, Egan JJ, et al. An official ATS/ERS/JRS/ALAT statement: idiopathic pulmonary fibrosis: evidence-based guidelines for diagnosis and management. *Am J Respir Crit Care Med.* 2011;183:788–824.
8. Wynn TA. Integrating mechanisms of pulmonary fibrosis. *J Exp Med.* 2011;208: 1339–1350.
9. Meyer KC. The natural history and diagnosis of idiopathic pulmonary fibrosis: are we all on the same page? *Chest.* 2011;140:3–4.
10. Raghu G, Collard HR, Anstrom KJ, et al. Idiopathic pulmonary fibrosis: clinically meaningful primary endpoints in phase 3 clinical trials. *Am J Respir Crit Care Med.* 2012;185:1044–1048.
11. Latsi PI, du Bois RM, Nicholson AG, et al. Fibrotic idiopathic interstitial pneumonia: the prognostic value of longitudinal functional trends. *Am J Respir Crit Care Med.* 2003;168:531–537.
12. Flaherty KR, Mumford JA, Murray S, et al. Prognostic implications of physiologic and radiographic changes in idiopathic interstitial pneumonia. *Am J Respir Crit Care Med.* 2003;168:543–548.
13. Shin KM, Lee KS, Chung MP, et al. Prognostic determinants among clinical, thin-section CT, and histopathologic findings for fibrotic idiopathic interstitial pneumonias: tertiary hospital study. *Radiology.* 2008;249:328–337.
14. Sumikawa H, Johkoh T, Colby TV, et al. Computed tomography findings in pathological usual interstitial pneumonia: relationship to survival. *Am J Respir Crit Care Med.* 2008;177:433–439.
15. Kaufmann M, Pusztai L. Use of standard markers and incorporation of molecular markers into breast cancer therapy: consensus recommendations from an International Expert Panel. *Cancer.* 2011;117:1575–1582.
16. Alexandraki KI, Kaltsas G. Gastroenteropancreatic neuroendocrine tumors: new insights in the diagnosis and therapy. *Endocrine.* 2012;41:40–52.
17. Ellison DW. Childhood medulloblastoma: novel approaches to the classification of a heterogeneous disease. *Acta Neuropathol.* 2010;120:305–316.
18. Lee SH, Shim HS, Cho SH, et al. Prognostic factors for idiopathic pulmonary fibrosis: clinical, physiologic, pathologic, and molecular aspects. *Sarcoidosis Vasc Diffuse Lung Dis.* 2011;28:102–112.
19. King TE Jr, Brown KK, Raghu G, et al. BUILD-3: a randomized, controlled trial of bosentan in idiopathic pulmonary fibrosis. *Am J Respir Crit Care Med.* 2011; 184:92–99.

20. Zhang Y, Kaminski N. Biomarkers in idiopathic pulmonary fibrosis. *Curr Opin Pulm Med.* 2012;18:441–446.
21. Ambrosini V, Zompatori M, De Luca F, et al. ^{68}Ga-DOTANOC PET/CT allows somatostatin receptor imaging in idiopathic pulmonary fibrosis: preliminary results. *J Nucl Med.* 2010;51:1950–1955.
22. Win T, Lambrou T, Hutton BF, et al. ^{18}F-fluorodeoxyglucose positron emission tomography pulmonary imaging in idiopathic pulmonary fibrosis is reproducible: implications for future clinical trials. *Eur J Nucl Med Mol Imaging.* 2012;39: 521–528.
23. Groves AM, Win T, Screaton NJ, et al. Idiopathic pulmonary fibrosis and diffuse parenchymal lung disease: implications from initial experience with ^{18}F-FDG PET/CT. *J Nucl Med.* 2009;50:538–545.
24. Borie R, Fabre A, Prost F, et al. Activation of somatostatin receptors attenuates pulmonary fibrosis. *Thorax.* 2008;63:251–258.
25. Munger JS, Huang X, Kawakatsu H, et al. The integrin alpha v beta 6 binds and activates latent TGF beta 1: a mechanism for regulating pulmonary inflammation and fibrosis. *Cell.* 1999;96:319–328.
26. Puthawala K, Hadjiangelis N, Jacoby SC, et al. Inhibition of integrin alpha(v) beta6, an activator of latent transforming growth factor-beta, prevents radiation-induced lung fibrosis. *Am J Respir Crit Care Med.* 2008;177:82–90.
27. Xu MY, Porte J, Knox AJ, et al. Lysophosphatidic acid induces alphavbeta6 integrin-mediated TGF-beta activation via the LPA2 receptor and the small G protein G alpha(q). *Am J Pathol.* 2009;174:1264–1279.
28. Horan GS, Wood S, Ona V, et al. Partial inhibition of integrin alpha(v)beta6 prevents pulmonary fibrosis without exacerbating inflammation. *Am J Respir Crit Care Med.* 2008;177:56–65.
29. Hausner SH, DiCara D, Marik J, Marshall JF, Sutcliffe JL. Use of a peptide derived from foot-and-mouth disease virus for the noninvasive imaging of human cancer: generation and evaluation of 4-[^{18}F]fluorobenzoyl A20FMDV2 for in vivo imaging of integrin alphavbeta6 expression with positron emission tomography. *Cancer Res.* 2007;67:7833–7840.
30. Hausner SH, Abbey CK, Bold RJ, et al. Targeted in vivo imaging of integrin alphavbeta6 with an improved radiotracer and its relevance in a pancreatic tumor model. *Cancer Res.* 2009;69:5843–5850.
31. Saha A, Ellison D, Thomas GJ, et al. High-resolution in vivo imaging of breast cancer by targeting the pro-invasive integrin alphavbeta6. *J Pathol.* 2010;222: 52–63.
32. Card JW, Carey MA, Bradbury JA, et al. Gender differences in murine airway responsiveness and lipopolysaccharide-induced inflammation. *J Immunol.* 2006; 177:621–630.
33. Johnson KA. Imaging techniques for small animal imaging models of pulmonary disease: micro-CT. *Toxicol Pathol.* 2007;35:59–64.
34. Tatler AL, John AE, Jolly L, et al. Integrin alphavbeta5-mediated TGF-beta activation by airway smooth muscle cells in asthma. *J Immunol.* 2011;187:6094–6107.
35. Hahm K, Lukashev ME, Luo Y, et al. Alphav beta6 integrin regulates renal fibrosis and inflammation in Alport mouse. *Am J Pathol.* 2007;170:110–125.
36. Wang B, Dolinski BM, Kikuchi N, et al. Role of alphavbeta6 integrin in acute biliary fibrosis. *Hepatology.* 2007;46:1404–1412.
37. Popov Y, Patsenker E, Stickel F, et al. Integrin alphavbeta6 is a marker of the progression of biliary and portal liver fibrosis and a novel target for antifibrotic therapies. *J Hepatol.* 2008;48:453–464.
38. Koth LL, Alex B, Hawgood S, et al. Integrin beta6 mediates phospholipid and collectin homeostasis by activation of latent TGF-beta1. *Am J Respir Cell Mol Biol.* 2007;37:651–659.
39. Wang A, Yokosaki Y, Ferrando R, Balmes J, Sheppard D. Differential regulation of airway epithelial integrins by growth factors. *Am J Respir Cell Mol Biol.* 1996;15:664–672.
40. Breuss JM, Gillett N, Lu L, Sheppard D, Pytela R. Restricted distribution of integrin beta 6 mRNA in primate epithelial tissues. *J Histochem Cytochem.* 1993; 41:1521–1527.
41. Larjava H, Koivisto L, Hakkinen L, Heino J. Epithelial integrins with special reference to oral epithelia. *J Dent Res.* 2011;90:1367–1376.
42. Huang XZ, Wu JF, Cass D, et al. Inactivation of the integrin beta 6 subunit gene reveals a role of epithelial integrins in regulating inflammation in the lung and skin. *J Cell Biol.* 1996;133:921–928.
43. Häkkinen L, Koivisto L, Gardner H, et al. Increased expression of beta6-integrin in skin leads to spontaneous development of chronic wounds. *Am J Pathol.* 2004;164:229–242.
44. Utz JP, Ryu JH, Douglas WW, et al. High short-term mortality following lung biopsy for usual interstitial pneumonia. *Eur Respir J.* 2001;17:175–179.
45. Committee HPAGBAoRSA. *Notes for Guidance on the Clinical Administration of Radiopharmaceuticals and the Use of Sealed Radioactive Sources*. Chilton, Didcot, Oxfordshire, U.K.: Health Protection Agency; 2006.
46. Krenning EP, Bakker WH, Kooij PP, et al. Somatostatin receptor scintigraphy with indium-111-DTPA-D-Phe-1-octreotide in man: metabolism, dosimetry and comparison with iodine-123-Tyr-3-octreotide. *J Nucl Med.* 1992;33:652–658.